(2)

AD-A254 955

DOCUMENTATION PAGE

Form Approved
OMB No. 0704-0188

1(A)	2. REPORT DATE	3. REPORT TYPE AND DATES COVERED
	24 July 1992	Reprint

4. TITLE AND SUBTITLE
The Semiannual Variation of Great Geomagnetic Storms and the Postshock Russell-McPherron Effect Preceding Coronal Mass Ejecta

5. FUNDING NUMBERS
PE 61102F
PR 2311
TA G4
WU 02

6. AUTHOR(S)
N.U. Crooker*, E.W. Cliver, B.T. Tsurutani#

7. PERFORMING ORGANIZATION NAME(S) AND ADDRESS(ES)
Phillips Lab/GPSG
Hanscom AFB
Massachusetts 01731-5000

8. PERFORMING ORGANIZATION REPORT NUMBER
PL-TR-92-2182

9. SPONSORING/MONITORING AGENCY NAME(S) AND ADDRESS(ES)

10. SPONSORING/MONITORING AGENCY REPORT NUMBER

11. SUPPLEMENTARY NOTES *Phillips Lab-on leave from Department of Atmospheric Sciences, UCLA, Los Angeles, CA 90024 #Jet Propulsion Laboratory, California Institute of Technology, Pasadena, CA 91109 - Reprinted from Geophysical Research Letters, Volume 19, No. 5, pages 429-432, March 3, 1992

12a. DISTRIBUTION/AVAILABILITY STATEMENT
Approved for public release; Distribution unlimited

12b. DISTRIBUTION CODE

13. ABSTRACT (Maximum 200 words)

Abstract. The occurrence rate of great geomagnetic storms displays a pronounced semiannual variation. Of the forty-two great storms during the period 1940-1990, none occurred during the solstitial months of June and December, and 40% (17) occurred during the equinoctial months of March and September. This suggests that the semiannual variation found by averaging indices is not the result of some statistical effect superposed on the effects of random storm occurrence but rather is dominated by the storms themselves. Recent results indicate that the intense southward interplanetary magnetic fields (IMFs) responsible for great storms can reside in the postshock plasma preceding the driver gas of coronal mass ejections (CMEs) as well as in the driver gas itself. Here we propose that strong southward fields in the postshock flow result from a major increase in the Russell-McPherron polarity effect through a systematic pattern of compression and draping within the ecliptic plane. Differential compression at the shock increases the Parker spiral angle and, consequently, the azimuthal field component that projects as a southward component onto Earth's dipole axis. The resulting prediction is that southward fields in the postshock plasma maximize at the spring (fall) equinox in CMEs emerging from toward (away) sectors. This pattern produces a strong semiannual variation in postshock IMF orientation and may account at least in part for the observed semiannual variation of the occurrence of great geomagnetic storms.

92-20709

92 7 30 040

14. SUBJECT TERMS
Geomagnetic storms, Semi-annual variation, In-ecliptic draping

15. NUMBER OF PAGES
4

16. PRICE CODE

17. SECURITY CLASSIFICATION OF REPORT	18. SECURITY CLASSIFICATION OF THIS PAGE	19. SECURITY CLASSIFICATION OF ABSTRACT	20. LIMITATION OF ABSTRACT
Unclassified	Unclassified	Unclassified	SAR

PL-TR-92-2182

GEOPHYSICAL RESEARCH LETTERS, VOL. 19, NO. 5, PAGES 429-432, MARCH 3, 1992

THE SEMIANNUAL VARIATION OF GREAT GEOMAGNETIC STORMS AND THE POSTSHOCK RUSSELL-MCPHERRON EFFECT PRECEDING CORONAL MASS EJECTA

N. U. Crooker[1,2], E. W. Cliver[1], and B. T. Tsurutani[3]

Abstract. The occurrence rate of great geomagnetic storms displays a pronounced semiannual variation. Of the forty-two great storms during the period 1940-1990, none occurred during the solstitial months of June and December, and 40% (17) occurred during the equinoctial months of March and September. This suggests that the semiannual variation found by averaging indices is not the result of some statistical effect superposed on the effects of random storm occurrence but rather is dominated by the storms themselves. Recent results indicate that the intense southward interplanetary magnetic fields (IMFs) responsible for great storms can reside in the postshock plasma preceding the driver gas of coronal mass ejections (CMEs) as well as in the driver gas itself. Here we propose that strong southward fields in the postshock flow result from a major increase in the Russell-McPherron polarity effect through a systematic pattern of compression and draping within the ecliptic plane. Differential compression at the shock increases the Parker spiral angle and, consequently, the azimuthal field component that projects as a southward component onto Earth's dipole axis. The resulting prediction is that southward fields in the postshock plasma maximize at the spring (fall) equinox in CMEs emerging from toward (away) sectors. This pattern produces a strong semiannual variation in postshock IMF orientation and may account at least in part for the observed semiannual variation of the occurrence of great geomagnetic storms.

Introduction

Geomagnetic storms, defined as periods of strengthened ring current in the inner magnetosphere, correlate remarkably well with southward excursions of the interplanetary magnetic field (IMF) [e.g., Burton et al., 1975]. Thus predicting storms becomes a matter of predicting IMF orientation. In general storms are attributed to two heliospheric features- recurrent stream interaction regions and transient coronal mass ejections (CMEs). The latter, when ejected fast enough to form a shock wave, produce the largest storms. For example, Gosling et al. [1991] find that 13 of the 14 largest storms as measured by K_p were caused by CMEs with shocks. Tsurutani et al. [1988, 1992] demonstrate that the southward fields that are the direct cause of CME-driven storms reside either in the postshock plasma that precedes the driver gas or in the driver gas itself or both. To predict the largest storms, then, one wishes to predict the orientation of the IMF in the postshock plasma and driver gas of fast CMEs.

A clue to predicting IMF orientation in postshock plasma and driver gas comes from the semiannual variation of large storms. The next section documents the remarkable strength of this variation. The following section demonstrates how the semiannual variation can arise from the heliospheric ordering of postshock flow and gives a scheme for predicting IMF orientation there. The final section discusses other possible contributions to the semiannual variation, including IMF orientation in the driver gas.

[1]Phillips Laboratory, Geophysics Directorate, Hanscom Air Force Base, MA 01731

[2]on leave from Department of Atmospheric Sciences, UCLA, Los Angeles, CA 90024

[3]Jet Propulsion Laboratory, California Institute of Technology, Pasadena, CA 91109

Paper number 92GL00377
0094-8534/92/92GL-00377$03.00

Semiannual Variation of Large Geomagnetic Storms

The semiannual variation of geomagnetic activity is well known and has been analyzed by a number of methods (see, e.g., Crooker and Siscoe [1986a] or Gonzalez et al. [1992] for review). It is usually treated as a statistical effect and attributed to a mechanism that gives stronger solar wind - magnetosphere coupling, on the average, in spring and fall. For example, Russell and McPherron [1973] attribute the semiannual variation to the fact that the average IMF, oriented at the Parker spiral angle in the solar equatorial plane, projects a southward component at Earth in the coupling-effective geocentric solar magnetospheric coordinate system whenever its polarity points toward the sun in spring and away from the sun in fall. The southward component achieved by this projection at equinox ranges from 28% to 40% of the IMF field strength, depending upon universal time.

Less known is the fact that the occurrence rate of large geomagnetic storms also shows a semiannual variation, which cannot be explained by the effects of average fields. Newton [1948] points out that the monthly distribution of great storms at Greenwich-Abinger during the period 1875-1946 has marked peaks in spring and fall. Figure 1a shows a histogram of the data used by Newton, updated to 1954 [Jones, 1955]. Of the total 112 great storms, 30% occurred in the peak equinoctial months of March and August and 6% during the solstitial months of June and December. Even the subset of the 11 most outstanding storms shows a semiannual variation. Allen [1982] obtains a similar result by plotting the monthly distribution of major storms determined by the parameter $A_p^* \geq 80$ during the period 1932-1980 [see, also, Gonzalez et al., 1992]. Figure 1b updates his result and restricts it to larger storms, with $A_p^* \geq 100$, during the period 1932-1989. Of the total 140 storms, 33% occurred in the peak equinoctial months of March and September, and 3.5% in the solstitial months of June and December (all in June).

Finally, Figure 1c gives the monthly distribution of great storms defined by the limit $D_{st} \leq -250$ nT, following Tsurutani et al. [1992]. Since D_{st} dates back only to 1957, we extend the list of storms to include the period from 1932 by using the index A_p^* as a proxy for D_{st} prior to 1957 in the following manner. For storms with $D_{st} \leq -250$ nT during 1957-1990, 72% (18/25) have $A_p^* \geq 160$. Conversely, of storms with $A_p^* \geq 160$ during this period, 69% (18/26) have $D_{st} \leq -250$ nT. Thus we choose $A_p^* \geq 160$ as a reasonable measure of great D_{st} storms for years prior to 1957 and lengthen the list from 25 to 42 cases. Of these, 40% occurred during the peak equinoctial months of March and September, and none during the solstitial months of June and December.

The pronounced semiannual variation in the histograms in Figure 1 does not arise as the result of large storms occurring randomly from one year to the next in one or the other of the equinoctial periods. Rather, the variation is remarkably well-defined even within single

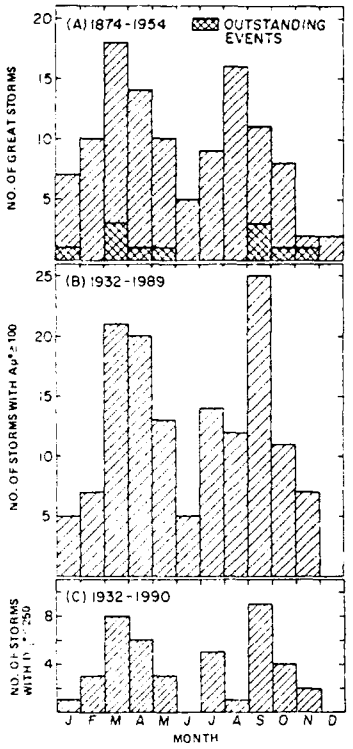

Fig. 1. The semiannual variation of the occurrence of great geomagnetic storms a.) with D range > 60′ or H or Z range > 300 nT at Greenwich or Abinger [Jones, 1955], b.) as measured by $A_p^* \geq 100$ nT, and c.) by $D_{st} \leq -250$ nT, after Tsurutani et al. [1992]. The "*" indicates that $A_p^* \geq 160$ nT was used as a proxy for D_{st} prior to 1957.

years that have large storms. Figure 2 demonstrates this fact with plots of the variation of monthly averages of D_{st} for those years when any single monthly average is ≤ -50 nT. In all three cases, there are pronounced peaks near both equinoxes. The phase varies from year

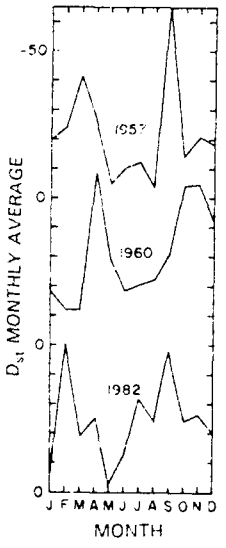

Fig. 2. The semiannual variation of monthly averages of D_{st}, with scale inverted, for those years beginning with 1957 in which any monthly average was more negative than −50 nT.

to year–for example, the spring peak occurs in February, March, and April, in the years 1982, 1957, and 1960, respectively–but the overall clarity of the variation is preserved. Bartels [1963] finds similar patterns for the indices K_p and A_p during disturbed years. The variable phase, also found in the power spectral analysis of A_p [Gonzalez et al., 1992], may reflect the remnant of CME occurrence variability after modulation by the mechanism that creates the semiannual wav..

The results in Figures 1 and 2 demonstrate semiannual variations with amplitudes that far exceed those obtained by averaging magnetic indices over many years. For example, Legrand and Simon [1989] point out that the semiannual variation in the *aa* index averaged over the period 1868-1980 has an amplitude equal to 13.5% of the average activity level, whereas the occurrence frequency of severe storms, defined by *Aa* (daily sum of *aa*) > 100 nT, shows a modulation of 80-90%. This amplitude difference, as well as the fact that individual years that have great storms show the most pronounced semiannual variation, as in Figure 2, imply that storms are responsible for most of the semiannual variation, rather than its being a statistical effect that one can sift out of the data by averaging over the effects of random storm occurrence. Green [1984] reaches the same conclusion based on his analysis of monthly averages of *aa*, designated A_a. He shows that the amplitude of the semiannual variation increases with increasing A_a and that its modulation in time is nearly identical to the time modulation of the amplitude of the semiannual variation in A_a occurrence for stormy days ($A_a > 30$). Although the semiannual variation is apparent at all levels of activity [e.g., Bartels, 1963; Green, 1984; Gonzalez et al., 1992], its dominance at high levels clearly indicates that some mechanism operates to occasionally produce very strong southward IMF at equinox and not at solstice.

Postshock Magnetic Field

Figure 3 presents a schematic drawing of the cross-section of a coronal mass ejection (CME) deforming the spiral magnetic field pattern in the ecliptic plane as it moves outward from the sun faster than the ambient medium. The CME presumably emerged from a helmet streamer [e.g., Hundhausen, 1988] and expands into the solar wind along a sector boundary, marked by the heliospheric current sheet (HCS) dividing fields pointing away from and toward the sun. Because of the spiral field

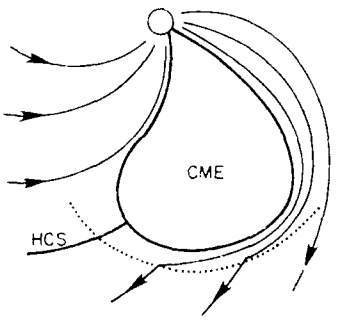

Fig. 3. Cross-section in the ecliptic plane of a coronal mass ejection (CME) expanding into the heliosphere along a sector boundary, marked by the heliospheric current sheet (HCS). Spiral magnetic field lines from the leading sector bend at the shock and drape around the CME, effecting an increase in the Parker spiral angle and the field strength in the postshock region.

geometry, the leading edge of the CME becomes mostly that portion west of its intersection with the HCS (see, also, Gosling et al. [1987]). The shock wave, represented by a dotted line, compresses the component of the spiral field that lies perpendicular to the shock normal. Thus it increases the Parker spiral angle as well as the total strength of the field from the leading sector across most of the leading edge of the CME. Further field intensification takes place from the shock to the CME boundary as the field stretches around the oncoming CME, in analogy with magnetic field behavior in Earth's magnetosheath [e.g., Crooker et al., 1982].

Figure 4 shows the IMF draped over the CME viewed toward the sun. The pattern is taken from the model calculated for Earth's magnetosheath with an upstream IMF directed 30° from the Earth-sun line [Crooker et al., 1985]. (A pattern for the 45° Parker spiral angle at Earth is not available.) The length of each vector is proportional to field strength. The arrowheads have been omitted so that one can use the diagram to represent either toward or away polarity. Earth's position could be anywhere relative to the CME but is shown as a dot on the CME's ecliptic equator near the region of maximum field strength. The draped field there lies in the geocentric solar ecliptic (GSE) X-Y plane, primarily in the Y_{GSE} direction (parallel to the solar equatorial Y direction at equinox). Earth's Z axis in geocentric solar magnetospheric (GSM) coordinates is tilted by the maximum value of 35° in the sense appropriate for September equinox at 1030 UT. For an IMF directed away from the sun, as in Figure 3, and as indicated by the large horizontal vector in Figure 4, its projection onto the Z_{GSM} axis provides a southward component equal to 57% of the Y_{GSE} component, which, according to Figure 3, is nearly the entire IMF vector. Thus the Russell-McPherron [1973] effect, applied to the geometry of the postshock field preceding a CME, provides a much stronger southward IMF component than in its original application to the average Parker spiral field. From it one can predict that postshock plasma will be geoeffective in northern hemisphere spring (fall) upon approach

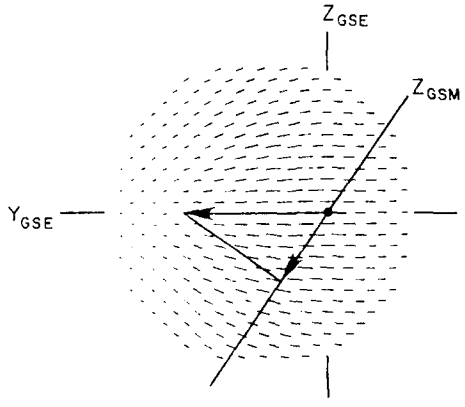

Fig. 4. View toward the sun of an array of magnetic field vectors draped over an approaching CME, from the magnetosheath draping model of Crooker et al. [1985]. Superposed on the array are vectors illustrating the postshock Russell-McPherron effect. From Earth, marked by a dot, extends a vector pointing in the Y_{GSE} direction representing the compressed, draped field preceding the CME in Figure 3. Its projection onto the Z_{GSM} axis, shown tilted the maximum of 35° from the GSE system in the sense appropriate for September equinox, forms a geoeffective southward component.

to toward-to-away (away-to-toward) sector boundaries, assuming CMEs emerge from helmet streamers there, as in Figure 3. Without this assumption, the prediction still holds for CMEs from toward sectors in spring and away sectors in fall.

It is important to note that the draping invoked here to produce southward IMF concerns only those fields lying in the ecliptic plane, in contrast to the proposal by Gosling and McComas [1987] that draping lifts the ambient field out of the ecliptic to produce southward IMF. Models of Earth's magnetosheath field indicate that substantial out-of-the-ecliptic components arise only when the IMF is nearly radial [Kartelev and Mastikov, 1982; Crooker et al., 1985]. For exactly radial IMF, the field diverges from the nose of the magnetosphere, or CME, in this case, and drapes directly upward and downward in the meridian plane containing the nose, as pictured by Gosling and McComas. However, for the IMF spiral angle of 30° used to construct Figure 4, the divergence point in the field pattern against the CME surface has moved off to the left, leaving draped field vectors lying mostly parallel to the ecliptic plane, especially in the region of maximum field strength. Since at Earth's orbit the ambient field has a spiral angle of 45°, that is, somewhat less radial than the 30° angle used for Figure 4, the draped fields should align even more with the ecliptic plane than illustrated. On the other hand, as noted by McComas et al. [1989], the ratio of radial-to-ecliptic components does increase somewhat with distance from the magnetopause or CME surface. But the continued dominance of the ecliptic component out to the shock leads us to conclude that the importance of out-of-the-ecliptic draping must be at most secondary, at least near equinox, compared to the Russell-McPherron effect, especially since only the latter can contribute to the semiannual variation of storm occurrence.

Discussion

The preceding section demonstrates how strong southward IMF can arise from compressed ecliptic fields in the postshock flow of CMEs during equinox. By themselves, these fields could be responsible for the pronounced semiannual variation in great geomagnetic storms. However, they may also serve as stepping stones to the generation of great storms during equinox by priming Earth's ring current so that additional southward fields in the driver gas carry D_{st} over the 250 nT threshold. Priming by postshock fields occurs in four of the ten less intense storms ($D_{st} \leq 100$ nT) analyzed by Tsurutani et al. [1988] with solar wind data, and the compound nature of the D_{st} profile for two-thirds of the great storms listed by Cliver et al. [1992] suggests that priming may be even more important for the largest storms. Thus, the postshock Russell-McPherron effect may serve as the added factor that brings storms up to great storm status.

Yet whether or not the postshock Russell-McPherron effect can account for the whole of the pronounced semiannual variation in great storm occurrence is not clear. Tsurutani et al. [1992] find that two of their five great storms are caused by driver gas alone. If driver gases alone are responsible for a large fraction of all great storms, as suggested by the limited study, then it seems that the occurrence frequency of driver gas storms must necessarily also have a semiannual variation, in order to account for the fact that essentially no great storms occur at the solstices. The only other possibility is that the magnetosphere itself loses its coupling efficiency at solstices [e.g., Crooker and Siscoe, 1986b].

A way in which driver gas storms may contribute to the semiannual variation is by retention of some of the ordered coronal fields in CMEs. Hoeksema and

Zhao [1992] demonstrate that field orientation retention appears to hold for four out of five cases of driver-gas-driven storms analyzed by Tsurutani et al. [1988, 1992]. Theoretically, if CMEs emerge from helmet streamers at sector boundaries with high inclination, as pictured in Figure 3, and the helmet fields form the leading edge of the driver gas [e.g., Hundhausen, 1988], then the leading edge will have roughly the same orientation as the overlying draped fields and, like them, be subject to the Russell-McPherron effect. The fact that sector boundaries tend to have high inclination near solar maximum [Hoeksema and Scherrer, 1986], when CME occurrence is highest [e.g., Webb, 1991], gives weight to the argument. Unfortunately, the limited amount of interplanetary data available for great storms hampers direct testing of this hypothesis.

Conclusions

1. The semiannual variation of great geomagnetic storm occurrence and of monthly avarages of D_{st} in years of great storms is remarkably pronounced. This implies that the semiannual variation found by averaging indices over many years is not a statistical effect superposed upon random storm occurrence but primarily the effect of the storms themselves.

2. Compression and draping within the ecliptic plane in postshock flow preceding CMEs greatly strengthens the Russell-McPherron effect there, which can account at least in part for the semiannual variation of great magnetic storm occurrence.

3. Whether or not geomagnetic storms caused by southward magnetic fields within the CME driver gas contribute to the semiannual variation remains to be tested.

Acknowledgements. The authors thank G. L. Siscoe for helpful discussion and R. Sagalyn for organizing a workshop in January, 1990, which stimulated the study. This research was supported in part by the Air Force Office of Scientific Research's University Resident Research Program. Portions were performed at the Jet Propulsion Laboratory, California Institute of Technology, under contract with the National Aeronautics and Space Administration.

References

Allen, J. H., Some commonly used magnetic activity indices: Their derivation, meaning and use, in *Proceedings of a Workshop on Satellite Drag*, March 1982, NOAA Space Environment Laboratory, Boulder, CO, 1982.

Bartels, J., Discussion of time-variations of geomagnetic activity, indices K_p and A_p, 1932-1961, *Ann. Geophys., 19,* 1-20, 1963.

Burton, R. K., R. L. McPherron, and C. T. Russell, An empirical relationship between interplanetary conditions and D_{st}, *J. Geophys. Res., 80,* 4204-4214, 1975.

Cliver, E. W., N. U. Crooker, and H. V. Cane, The semiannual variation of great geomagnetic storms: Solar sources of great storms, Proceedings of the First SolTip Symposium, Liblice, Czechoslovakia, 1991, in press, 1992.

Crooker, N. U., and G. L. Siscoe, The effect of the solar wind on the terrestrial environment, in *Physics of the Sun,* edited by P. A. Sturrock, pp. 193-249, D. Reidel, Hingham, Mass., 1986a.

Crooker, N. U., and G. L. Siscoe, On the limits of energy transfer through dayside merging, *J. Geophys. Res., 91,* 13393-13397, 1986b.

Crooker, N. U., et al., Magnetic field compression at the dayside magnetopause, *J Geophys. Res., 87,* 10407-10412, 1982.

Crooker, N. U., et al., Magnetic field draping against the dayside magnetopause, *J. Geophys. Res., 90,* 3505-3510, 1985.

Gonzalez, A. L. C., W. D. Gonzalez, S. L. G. Dutra, and B. T. Tsurutani, Periodic variation in the geomagnetic activity: A study based on the A_p index, *J. Geophys. Res.,* submitted, 1992.

Gosling, J. T., and D. J. McComas, Field line draping about fast coronal mass ejecta: A source of strong out-of-the-ecliptic interplanetary magnetic fields, *Geophys. Res. Lett., 14,* 355-358, 1987.

Gosling, J. T., et al., The eastward deflection of fast coronal mass ejecta in interplanetary space, *J. Geophys. Res., 92,* 12399-12406, 1987.

Gosling, J. T., et al., Geomagnetic activity associated with earth passage of interplanetary shock disturbances and coronal mass ejections, *J. Geophys. Res., 96,* 7831-7839, 1991.

Green, C. A., The semiannual variation in the magnetic activity indices A_a and A_p, *Planet. Space Sci., 32,* 297-305, 1984.

Hoeksema, J. T., and P. H. Scherrer, The solar magnetic field-1976 through 1985, Report UAG-94, World Data Center A for Solar-Terrestrial Physics, Boulder, CO, 1986.

Hoeksema, J. T., and X. Zhao, Prediction of magnetic orientation in driver gas - associated -Bz events, *J. Geophys. Res.,* in press, 1992.

Hundhausen, A. J., The origin and propagation of coronal mass ejections, in *Proceedings of the Sixth International Solar Wind Conference,* edited by V. J. Pizzo, T. E. Holzer, and D. G. Sime, NCAR/TN-306+Proc, pp. 181-214, Boulder, CO, 1988.

Jones, H. S., *Sunspot and Geomagnetic-Storm Data Derived from Greenwich Observations,* 1874-1954, pp. 71-82, Royal Greenwich Observatory, Her Majesty's Stationery Office, London, 1955.

Kartalev, M. D., and I. P. Mastikov, Steady-state magnetic field in the magnetosheath, *Planet. Space Sci., 30,* 473-481, 1982.

Legrand, J.-P., and P. A. Simon, Solar cycle and geomagnetic activity: A review for geophysicists. Part I. The contributions to geomagnetic activity of shock waves and of the solar wind, *Ann. Geophys., 7,* 565-578, 1989.

McComas, D. J., et al., A test of magnetic field draping induced B_z perturbations ahead of fast coronal mass ejecta, *J. Geophys. Res., 94,* 1465-1471, 1989.

Russell, C. T., and R. L. McPherron, Semiannual variation of geomagnetic activity, *J. Geophys. Res., 78,* 92-108, 1973.

Tsurutani, B. T., et al., Origin of interplanetary southward magnetic fields responsible for major magnetic storms near solar maximum (1978-1979), *J. Geophys. Res., 93,* 8519-8531, 1988.

Tsurutani, B. T., et al., Great magnetic storms, *Geophys. Res. Lett., 19,* 73-76, 1992.

Webb, D. F., The solar cycle variation of the rates of CMEs and related activity, *Adv. Space Res., 11,* (1)37-(1)40, 1991.

E. W. Cliver, Phillips Laboratory/GPSG, Hanscom Air Force Base, MA 01731

N. U. Crooker, Department of Atmospheric Sciences, UCLA, Los Angeles, CA 90024-1565

B. T. Tsurutani, Jet Propulsion Laboratory, California Institute of Technology, Pasadena, CA 91109

Received: November 11, 1991
Revised: December 30, 1991
Accepted: January 21, 1992